

FEDSM99-6761

## COMPUTATIONS OF TURBULENT MIXING AT THE INTERFACE OF A DENSITY STRATIFIED, SHEAR LAYER

Ismail B. Celik, Matthew R. Umbel, and Wesley M. Wilson  
Mechanical and Aerospace Engineering Department  
West Virginia University  
Morgantown, WV 26506-6106  
Phone: (304) 293-3111, Ext. 325  
Fax: (304) 293-6689  
Email: [icelik@wvu.edu](mailto:icelik@wvu.edu)

### ABSTRACT

Several numerical simulations were performed of a developing shear layer involving miscible and immiscible fluids. The objective was to refine a simplified model and demonstrate its predictive capability of trends for such parameters as the mixed fluid thickness and gradient Richardson number along the shear layer. Time-averaged, steady state solutions were obtained using a single fluid, scalar transport (SFST) model, which is a variant of the so called drift flux model. The standard  $k-\epsilon$  turbulence model was used with additional terms to account for the influences of buoyancy production/destruction. Mixing at the interface of two miscible fluids was studied in light of the experiments by Sullivan and List (1994). Here the primary concern was the prediction of interfacial mixing or entrainment of one fluid into the other. Next, the experiments being conducted at Johns Hopkins University using diesel fuel and water were simulated. Here the rise or settling velocity of the fuel droplets has a significant effect on interface mixing; hence, the ability to account for relative or slip velocity effects was investigated. Comparison with preliminary experimental results indicates that the simulations produce good results with regard to the overall averaged flowfield and mixed fluid thickness.

### INTRODUCTION

The present study is an element of a larger work being conducted at West Virginia University and the Naval Surface Warfare Center – Carderock Division (NSWC-CD) in Bethesda, MD, to study the transient flow phenomena that occur during the refueling of compensated fuel/ballast tanks (CFBT's), which are used in U.S. naval surface ships. Of primary interest in these studies is the location and extent of

fuel/water mixing, the amount of water trapped (water hideout) in the tanks after refueling is complete, and the estimated flow-through time of the fuel. To aid in this study, numerical simulations are currently being performed, in parallel with experimental work being conducted at Johns Hopkins University, to assess flow characteristics and mixing parameters during the shearing flow of two immiscible fluids. These simulations are of practical importance in understanding fuel/water mixing and general flow characteristics in the interior of CFBT compartments where diesel fuel flows over a more dense layer of seawater. The two-fluid flows inside CFBT's are characterized by stratified shear layers, buoyant jets, and impinging jets. In the first phase of this ongoing study only shear layers are considered.

In characterizing stratified shear flows, most experiments (see e.g. Fernando, 1991) describe several interfacial mixing regimes that depend on the relative influence of buoyancy and turbulence at the interface, which in turn can be described by a characteristic Richardson number. For very low values of the Richardson number, a regime is defined in which mixing is primarily caused by interfacial instabilities that are commonly observed in constant density flows where the interface is fully turbulent. This interface is regarded to show a significant Reynolds number dependence as the flow situation is very similar to flows without density stratification. As the Richardson number is increased, the turbulence at the interface is damped and the mixing is primarily due to Kelvin-Helmholtz type waves, which thicken the interface by periodic formation and breaking. At still larger Richardson numbers, the interfacial mixing is driven by interfacial waves, which form and are sheared off by the ambient turbulent eddies; here

an eddy from the homogeneous layer scours the surface of the mixed interface and draws fluid of greater density into a crest, which is then sheared off. At very high Richardson numbers, interfacial waves are suppressed and the mixing is dominated by molecular diffusion, which implies a Peclet number dependence as well.

For verification of the SFST model, numerical simulations have been performed in light of the experiments by Sullivan and List (1994). These experiments involved measurements of tracer dye concentrations in a homogeneous, density stratified, turbulent, shear flow. Following these verification studies, the experimental conditions for immiscible shear flow studies being performed at Johns Hopkins University were simulated. These experiments involve the flow of an upper layer of diesel fuel over a lower layer of fresh water. The results of the simulations were compared with experiments, both qualitatively and quantitatively, wherever possible.

## NOMENCLATURE

### English

b	Buoyancy ( $= g(\rho_\beta - \rho_\alpha)/\rho_\alpha$ )
E	Dimensionless entrainment velocity ( $= u_e/\Delta U$ )
$h_s$	Maximum velocity gradient thickness
h	Concentration boundary layer thickness
H	Total depth of upper and lower layers in shear flow
$H_0$	Lower layer vertical inlet height
$H_1$	Upper layer vertical inlet height
$H_2$	Lower layer vertical outlet height
$H_3$	Upper layer vertical outlet height
P	Modified pressure for turbulent flows
$Q_0$	Lower layer inlet flow rate per unit length
$Q_1$	Upper layer inlet flow rate per unit length
$Q_2$	Lower layer outlet flow rate per unit length
$Q_3$	Upper layer outlet flow rate per unit length
r	Volume fraction
$Ri_G$	Gradient Richardson number
$Ri_L$	Mixed layer Richardson number ( $= \delta_M b/(\Delta U)^2$ )
$Ri^*$	Overall Richardson number ( $= bH/(\Delta U)^2$ )
$u_e$	Entrainment velocity
$u_i$	Mean interface velocity
$U_S$	Slip or relative velocity between phase $\alpha$ and phase $\beta$

### Greek Symbols

$\delta$	Interfacial thickness
$\delta_M$	Mixed fluid thickness
$\rho$	Density
$\eta$	Mean interface position

### Subscripts

$\alpha$	Phase alpha (denotes lighter phase)
$\beta$	Phase beta (denotes heavier phase)

m	Indicates mixture quantity
1	Upper layer in homogeneous shear flow
0	Lower layer in homogeneous shear flow

## 2.0 METHODOLOGY

The numerical simulations were performed using a commercial CFD code, CFX-4, developed by AEA Technologies, with a user implemented mixture model to simulate the flow of the two fluids similar to Ishii's drift flux model (Ishii, 1975). The momentum equations are solved for the mixture as a whole, with variable density, and mixture definitions are used for the velocity, density, and viscosity based on the individual phase values. The present study adopts the definitions for the mixture quantities and the form of the individual phase mass and momentum equations as given by Ishii (1975). From these definitions and equations a model is developed for turbulent flows where two liquids mix and the relative velocity between the liquids is non-zero, as is typical for buoyant, immiscible flows (Umbel, 1998; Celik *et al*, 1998). This model is referred to as a single fluid, scalar transport (SFST) model. For cases where the relative velocity between the phases is negligible, the SFST model can be further simplified to give a model that is typically used for miscible fluids.

Three of the main assumptions that are used in formulating the SFST model are that the individual phases are incompressible, the flow is isothermal, and that the density difference between the phases is small compared to the density of either phase. These assumptions allow certain terms to be neglected in the model equations for turbulent flows. Another important assumption involves using a gradient diffusion model for the average turbulent stresses in the momentum equations and similarly for the turbulent transport terms in the scalar transport equations. The relative velocity (or slip) between the two phases is modeled using a constitutive equation, given by

$$u_S = f(r_a, \mathbf{r}_m, u_m, g, \text{etc.}) \quad (1)$$

This assumption is justified if the motion of the two phases is strongly coupled. A relatively simple model is to assume that the slip velocity is a function of the terminal velocity of an average size droplet and the local volume fraction to account for droplet-droplet interactions. In this study the slip velocity is calculated from

$$u_{s,i} = U_s d_{2i} \quad (2)$$

where  $\delta_{2i}$  is the Kronecker delta function,  $i=2$  is the vertical direction, and

$$U_s = \left( \frac{4d_p g}{3C_D} \right)^{1/2} \left( \frac{\mathbf{r}_b - \mathbf{r}_a}{r_b} \right)^{1/2} \quad (3)$$

where  $U_s$  is the slip velocity,  $d_p$  is the droplet diameter, and  $C_D$  is the drag coefficient. For more details of the model the reader is referred to Umbel (1998) and Celik et al (1998).

Unless otherwise stated, the convective terms were discretized using the Hybrid Scheme (mixed upwind & central) for all equations except the volume fraction equation, where only the upwind scheme was used. All other terms were approximated as central differences on co-located grids.

### 3.0 SFST MODEL PREDICTIONS FOR MISCIBLE FLUIDS

Sullivan and List (1994) performed experiments by measuring tracer dye concentrations in a homogeneous, density stratified, turbulent, shear flow. The flow scenario used in these experiments is shown schematically in Fig. 1. Here  $U$ ,  $h$ , and  $\rho$  denote the free stream velocity, concentration boundary layer, and unmixed density for each layer, where the top and bottom layers are denoted by 1 and 0 respectively. The experimental setup consisted of a counter flow that was generated by two inlets at the opposite ends of a 5.0 m long by 20.0 cm high by 10.0 cm wide laboratory channel (see Fig. 1).

The heavy fluid (aqueous saline solution) and the light fluid (aqueous ethanol solution) were separated by splitter plates at the inlets. Typical inlet flow rates were approximately  $40.0 \text{ cm}^3/\text{s}$  per unit width, corresponding to inlet velocities of approximately  $4.0 \text{ cm/s}$  and inlet Reynolds numbers of approximately 4,000 based on the inlet height. The buoyancy,  $b$ , ranged from  $5.0$  to  $20.0 \text{ cm/s}^2$ . These experiments were performed over a range of shear Richardson numbers varying from 0.1 to 1.0, which approximately corresponded to a Kelvin-Helmholtz and a shear driven, wave breaking mixing regime.

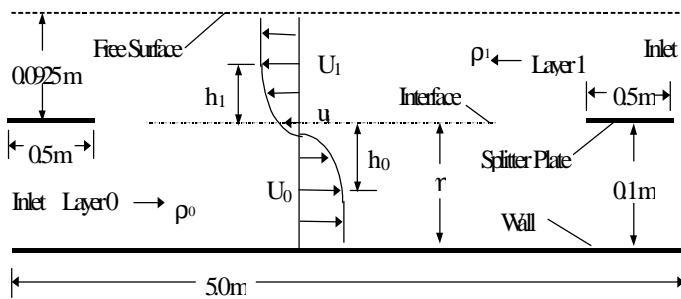


Figure 1 – Schematic of Sullivan and List experimental setup with idealized shear layer.

In the experiments, the mean interface velocity,  $u_i$ , was estimated by linear interpolation. In the present simulations  $u_i$  was linearly interpolated based on the location of the mean interface position as calculated by the code. An overall Richardson number, where  $H$  is the total height of the test section and  $\Delta U = (U_1 - U_0)$  was used to characterize the flow.

This Richardson number can be adjusted such that it is the same for the experiments and the simulations for comparative study. Four cases were simulated, corresponding to the experiments (Sullivan and List, 1994) labeled 1, 10, 11, and 13. The key parameters for these cases are given in Table 1.

Table 1 - Experimental Flow Parameters

Case	$b(\text{cm/s}^2)$	$Q_b(\text{cm}^2/\text{s})$	$Q(\text{cm}^2/\text{s})$	$H_b(\text{cm})$	$H_1(\text{cm})$	$H_2(\text{cm})$	$H_3(\text{cm})$
1	1881	3682	3897	1000	925	1000	925
10	1277	3874	3975	1000	925	1000	925
11	748	3874	2642	1000	925	1000	925
13	1895	3874	3975	1000	925	1000	925

A medium grid, consisting of  $450 \times 50$  cells, and a fine grid, consisting of  $600 \times 80$  cells, were used for the simulations. The cells were concentrated towards the lower wall and vertical center of the model using a geometric progression factor of 1.04. The smallest cell dimensions at the interface were approximately  $1.0 \text{ cm}$  long by  $2.0 \text{ mm}$  high and  $8.0 \text{ mm}$  long by  $1.0 \text{ mm}$  high, for the medium and fine grids, respectively. The QUICK scheme was used for convective terms in the momentum equations. All simulations were run as 2D turbulent flows using transient marching to steady state. Typically, 30 outer iterations were performed over about 500 time steps of 1.0 second, which corresponded to approximately three flow-through times. At this time, the outlet flowrates and vertical profiles of all the quantities remained constant with continued iteration and the solution was assumed to attain steady state.

Boundary conditions for the inlets were modeled by setting a fixed velocity such that the inlet flow rates were the same as those in the experiments. Specified values of the volume fractions corresponding to the pure unmixed fluids were also set at the inlets. Values of  $k$  and  $\epsilon$  were estimated at the inlets using

$$k_{inl} = c_{p1} U_{inl}^2 \quad ; \quad \epsilon_{inl} = \frac{k_{inl}}{c_{p2} D_h} \quad (4)$$

where  $c_{p1}$  and  $c_{p2}$  are empirical constants with values of 0.002 and 0.3 respectively, and  $D_h$  is the hydraulic diameter. The resulting turbulence intensity was approximately 5% of the inlet velocity. Dirichlet boundary conditions were specified on all quantities at the inlets, except pressure, which was extrapolated from downstream. Boundary conditions at the outlets were set as if the fluid was exiting the domain with a free surface at the top of the outlet boundary in the longitudinal direction, corresponding to atmospheric pressure at the top of the outlet boundary. For stratified flows exiting the domain, the discretized pressure is set by

$$p_j = p_{j+1} + \int_j^{j+1} (\mathbf{r}_m - \mathbf{r}_{Ref})(g)dy \quad (5)$$

and the  $j$  index indicates the vertical direction. Here  $\rho_{Ref}$  is a reference density, which was set equal to the average of the unmixed phase densities. A zero derivative condition was used for all other quantities at the outlets. The free surface was modeled as a plane of symmetry. Quantities as set at the inlets for each case are listed in Table 2.

Table 2 - Inlet Flow Parameters for CFX model

Lower inlet parameters

Case	U (cm/s)	V (cm/s)	$\rho$ (kg/m <sup>3</sup> )	$k$ (cm <sup>2</sup> /s <sup>2</sup> )	$\epsilon$ (cm <sup>2</sup> /s <sup>3</sup> )
1	3.682	0.00	1019.00	0.0271	0.0098
10	3.874	0.00	1013.00	0.0300	0.0108
11	3.874	0.00	1008.00	0.0300	0.0108
13	3.874	0.00	1019.00	0.0300	0.0108

Upper Inlet parameters

Case	U (cm/s)	V (cm/s)	$\rho$ (kg/m <sup>3</sup> )	$k$ (cm <sup>2</sup> /s <sup>2</sup> )	$\epsilon$ (cm <sup>2</sup> /s <sup>3</sup> )
1	4.213	0.00	1000.00	0.0355	0.0128
10	4.297	0.00	1000.00	0.0369	0.0133
11	2.856	0.00	1000.00	0.0163	0.0059
13	4.297	0.00	1000.00	0.0369	0.0133

### 3.1 RESULTS AND DISCUSSION

In the experiments, the interfacial mixing for cases 1 and 13 was characterized as belonging to the shear driven wave-breaking regime. For cases 10 and 11, the interfacial mixing was characterized by Kelvin-Helmholtz instabilities. The data used to calculate the desired flow parameters was taken along a vertical line at different locations in the longitudinal direction for each case. In the simulations, the data was taken at similar locations, corresponding to the appropriate case. Longitudinal averages of measured parameters were also calculated in the simulations; these averages were taken between 50.0 and 350.0 cm from the left splitter plate.

The mixed fluid thickness is used to measure the capability of the model to predict the overall mixing in the turbulent layer. The mixed layer Richardson number,  $Ri_L$ , is used to measure the relevant scales of buoyancy to turbulence in the layer. Figure 2 shows the predicted trend for this parameter as compared to the experiments. Given the simplicity of the present model and the uncertainty in measuring the interface velocity (Sullivan and List, 1994), the observed agreement is deemed satisfactory.

Another parameter related to the overall mixing in the two layers is the dimensionless entrainment velocity,  $E$ . The entrainment velocity,  $u_e$ , was calculated using the average of the amount of lower layer fluid flowing out of the domain

above  $\eta$  (mean interface position) per unit time and the amount of upper layer fluid flowing out of the domain below  $\eta$  per unit time, divided by the area over which entrainment occurred. A power law fit through the four data points gives  $E \sim Ri^{*-1.1}$ , with an exponent within the experimentally reported range. Typical experimental values for the exponent range from -0.5 to -2.0, depending on the experiment and the definition of the Richardson number (Fernando, 1991).

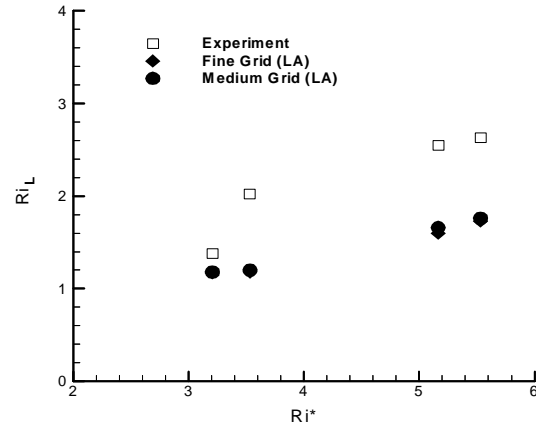


Figure 2 - Variation of  $Ri_L$  with  $Ri^*$ .

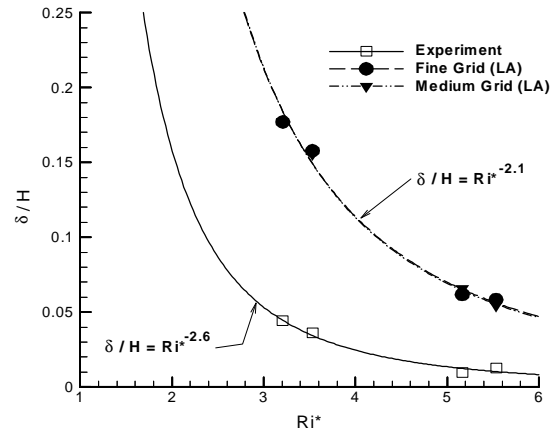


Figure 3 - Normalized interfacial thickness versus  $Ri^*$ .

The quantity  $\delta/H$  is plotted against the overall Richardson number in Fig. 3. The predicted trend for the average interfacial thickness,  $\delta$ , was good for all four cases, though the predicted magnitude was somewhat higher than the experimental values. For increasing density stratification, the interfacial thickness generally decreases according to some power law of the Richardson number. The power law as given by the simulations over the four data points gives a somewhat lower exponent.

In general the SFST model gave reasonable predictions for the majority of the relevant parameters. The interfacial parameters were the most difficult to predict, presumably

because of low Reynolds number effects that are not accounted for by the present form of the  $k-\epsilon$  model. These results were also partially polluted by poor performance of the  $k-\epsilon$  turbulence model near the free surface and near the walls. All other quantities, when considered in light of the longitudinal averages, were also well predicted in both trend and magnitude (see Umbel, 1998 for more details).

#### 4.0 PREDICTIONS FOR IMMISCIBLE FLUIDS

Steady state shearing flows involving diesel fuel and fresh water flowing in a laboratory channel apparatus were simulated using the suggested SFST model in conjunction with CFX-4. The simulations were based on a shear flow facility currently being used at Johns Hopkins University (Katz, 1998). Altogether, four cases were simulated where the overall Richardson number and the average droplet size, which was assumed to be constant in each case, were varied. Of primary interest in these simulations was the trend in the gradient Richardson number over the vertical shear layer and along the streamwise direction. The gradient Richardson number is a local parameter and can be helpful in describing local effects in the flow field. Trends for the interface thickness as functions of the maximum gradient Richardson number were studied as well. The gradient Richardson number is defined by

$$Ri_g = \frac{-(g/r)(\nabla r / \nabla y)}{(\nabla u / \nabla y)^2} \quad (7)$$

This parameter was used because the flow field that is generated in the shear flow apparatus is not homogeneous in the longitudinal direction; therefore, characterizing the state of the flow by a single Richardson number was difficult and hence a local parameter was deemed necessary.

The experimental setup consisted of essentially two stratified, immiscible, fluid layers flowing opposite to each other in a laboratory, channel apparatus (see Fig. 4), which was approximately 150.0 cm long, 32.0 cm high, and 7.5 cm wide. The water and fuel inlets were both 11.0 cm high. Fuel with a density of  $850.0 \text{ kg/m}^3$ , entered the apparatus from the upper left, while water, with a density of approximately  $1000.0 \text{ kg/m}^3$ , entered from the lower right at a significantly higher flow rate than the fuel. An inlet diffuser smoothly transitioned the fuel into the oncoming water, where the interface shear developed. Some of the fuel exited the domain through the top outlet into a fuel reservoir, while most of the fuel, which was entrained in the water, exited through the lower outlet. An outlet weir below the fuel inlet diffuser acted to direct the flow of water along the fuel interface.

The main shear region between the fuel-inlet diffuser and the water-inlet splitter plate was approximately 0.8 m in length. Typical inlet flow rates for the fuel were approximately

$0.00095 \text{ m}^3/\text{s}$  corresponding to a mean inlet velocity of  $0.115 \text{ m/s}$ . Inlet flow rates for the water ranged from  $0.0044$  to  $0.0075 \text{ m}^3/\text{s}$  corresponding to mean inlet velocities of  $0.54 \text{ m/s}$  to  $0.92 \text{ m/s}$ . The same definitions as were used for the Sullivan and List simulations were also used in describing this flow. The constitutive equation for the slip velocity was given by the terminal rise velocity of a single fluid droplet (Eq. 3).

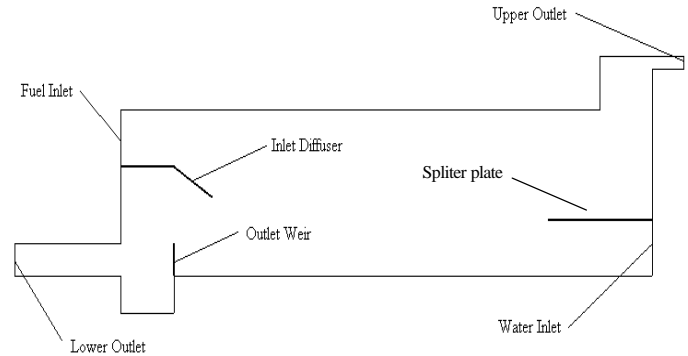


Figure 4 - Johns Hopkins shear flow experimental setup.

A fine grid consisting of 29,175 cells was used for the simulations. In the main shear region, between the splitter plates, the grid consisted of 150 cells in the longitudinal direction by 104 cells in the vertical direction. Here the cells were concentrated towards the lower wall and vertical center of the model using a geometric progression factor of 1.02. This gave the smallest cell at or near the interface dimensions of approximately  $5.0 \text{ mm}$  long by  $1.0 \text{ mm}$  high.

Boundary conditions for the inlets were modeled by setting a fixed velocity such that the overall Richardson number matched that based upon the flowrates used in the experiments. Specified values of the volume fractions corresponding to the pure unmixed fluids were also set at the inlets. Values of  $k$  and  $\epsilon$  were estimated at the inlets using Eq. (4), and pressure at the inlets was extrapolated from downstream. Boundary conditions at the outlets were set as described in Section 3.0. In addition to the hydrostatic distribution, a constant pressure of  $2586.0 \text{ Pa}$  was set at the upper right outlet, corresponding to a pressure difference of  $0.375 \text{ psi}$  between the top and bottom outlets. This was done since the fuel outlet tank on the right of the apparatus is typically pressurized in the experiments. Boundary conditions for all other quantities at the outlets were modeled by setting a zero derivative condition. Quantities as set at the inlets for each case are listed in Table 3.

All simulations were run using transient marching to steady state. Typically 50-75 outer iterations were performed over about 280 time steps of  $0.1 \text{ second}$ . This corresponded to approximately three flow-through times for the fuel and about 25 flow-through times for the water. At this time the outlet

flow rates and vertical profiles of all the quantities remained constant and the solution was taken as the steady state.

Table 3 - Inlet Flow Parameters and Case Specifics

Lower inlet parameters					Overall Parameters	
Case	u (cm/s)	$\rho$ (kg/m <sup>3</sup> )	k (cm <sup>2</sup> /s <sup>2</sup> )	$\epsilon$ (cm <sup>2</sup> /s <sup>3</sup> )	d <sub>p</sub> (mm)	Ri*
1	69.03	1000.00	9.530	3.434	1.75	1.29
2	69.03	1000.00	9.530	3.434	2.35	1.29
3	92.04	1000.00	16.943	6.105	1.75	0.51
4	92.04	1000.00	16.943	6.105	2.35	0.51

Upper Inlet parameters				
Case	u (cm/s)	$\rho$ (kg/m <sup>3</sup> )	k (cm <sup>2</sup> /s <sup>2</sup> )	$\epsilon$ (cm <sup>2</sup> /s <sup>3</sup> )
1	11.50	850.00	0.265	0.095
2	11.50	850.00	0.265	0.095
3	11.50	850.00	0.265	0.095
4	11.50	850.00	0.265	0.095

#### 4.1 RESULTS AND DISCUSSION

The velocity and volume fraction profiles at various x-locations are shown in Figs. 5 & 6.

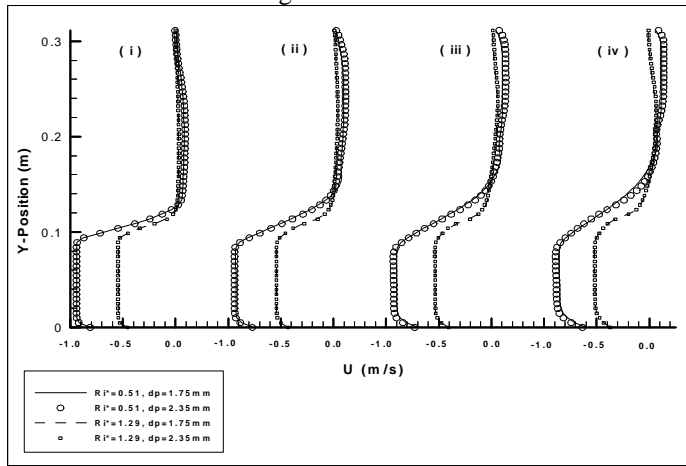


Figure 5 – U velocity profiles at x/L = (i) 0.2, (ii) 0.4, (iii) 0.6, and (iv) 0.8.

As expected, the mixed layer thickness decreases with increasing Ri\* and increasing mean droplet size. Figure 5 shows a much sharper interface for the larger Ri\* indicating the stabilizing effect of the buoyancy resulting from a stable density stratification. Figure 6 shows a similar trend with volume fraction profiles, from which the mixed fluid thickness,  $\delta_M$ , was calculated. The influence of droplet size (or slip velocity) on the velocity profiles is negligibly small. In contrast, the slip velocity shows a marked influence in the volume fraction profiles for the lower Ri\*, which is expected to give a fully turbulent interface. The interface sharpening effect of the slip velocity term is clearly seen in Fig. 6. The double-layer stratification observed in Fig. 6 at x/L = 0.6 & 0.8 is probably due to the recirculation region predicted in the simulations near the inlet diffuser.

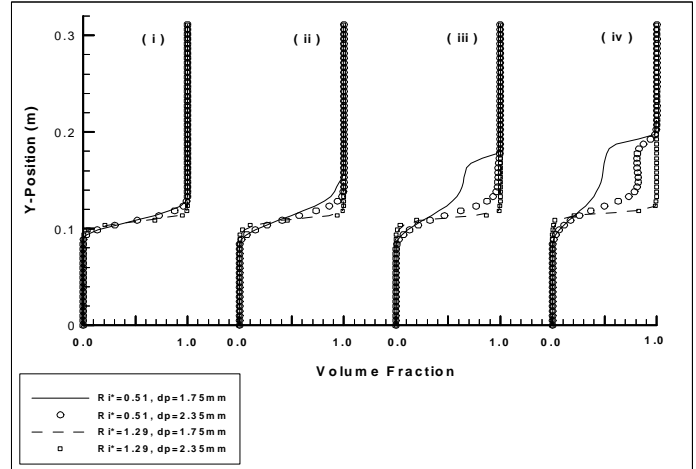


Figure 6 – Volume fraction profiles at x/L = (i) 0.2, (ii) 0.4, (iii) 0.6, and (iv) 0.8.

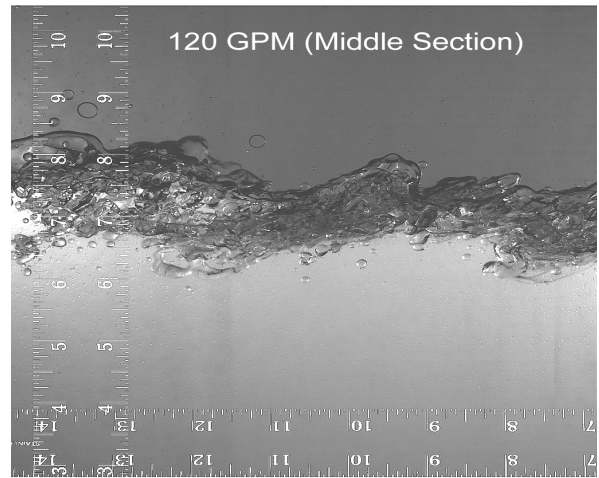


Figure 7 - Instantaneous mixing layer near central section; After Wu and Katz (1998). [flow from right to left]

A typical instantaneous image of the sheared interface was obtained from the shear flow facility at Johns Hopkins (Wu and Katz, 1998) and is reproduced in Fig. 7. The flow rate that was used in the experiments was 0.00757 m<sup>3</sup>/s (120 GPM) and corresponds approximately to the inlet velocities that were used in the simulations for cases 3 and 4, i.e. Ri\* = 0.59. Figure 7 clearly shows the droplets that are formed at the interface. The various sizes of the droplets that are formed can be inferred from this image and give some credibility to the choices that were made for the average droplet sizes in the simulations.

With regard to the shear at the interface, the zone of recirculation occurring just after and above the fuel inlet diffuser tends to disrupt part of the shear layer. This is especially evident for the cases where Ri\* is low. The existence of this large re-circulation zone was experimentally confirmed (Wu

and Katz, 1998), and will influence experimental data that is taken in the surrounding region.

The gradient Richardson number was calculated at various locations in the streamwise direction. For cases 1 & 3,  $Ri_G$  is shown at several  $x/L$  locations in Figs. 8 & 9.  $L$  is the distance between the tip of the fuel inlet diffuser and the right splitter plate. For the case where  $Ri^* = 0.51$  the profiles are only shown through  $x/L = 0.3$  since effects of the re-circulation zone were evident at larger  $x/L$  values.

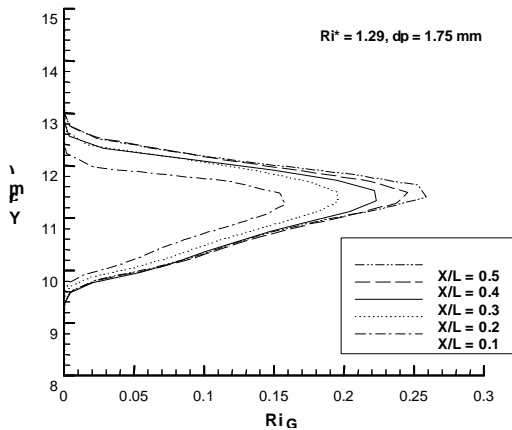


Figure 8 - Gradient Richardson number profiles for case 1.

It is seen from figs. 8 & 9 that  $Ri_G$  increases with  $x/L$ . This happens because of the velocity layer spreading and  $(\partial U/\partial y)^2$  decreasing more rapidly than  $\partial \rho/\partial y$ . The maximum value of  $Ri_G$  is a reasonable parameter to characterize the shear layer at various  $x/L$  locations. The vertical location of the maximum value of  $Ri_G$  can be taken as a measure of how the location of the interface,  $y_i$ , changes. Figures like 8 & 9 showed that  $y_i$  increases with decreasing  $Ri^*$  and  $d_p$ . The trend for the maximum gradient Richardson number is shown (Figs. 8 & 9) over a smaller range of  $x/L$  values for the cases where  $Ri^* = 0.51$ ; this was done to avoid the values that were influenced by the re-circulation zone. There is roughly an order of magnitude increase in  $(Ri_G)_{max}$  over the development of the shear layer; hence, flow regimes may change dramatically within the same experimental conditions.

Tennekes and Lumley (1972) comment that for typical shear flows turbulence will persist at the interface for  $Ri_G < 0.2$ . Miles (1984) comments that for unbounded, parallel shear flow, if  $Ri_G > 0.25$  then no turbulent instabilities are observed near the interface as all turbulent motion is damped by buoyancy. However, for bounded flows, the critical gradient Richardson number can be much lower than 0.25, and the value of  $Ri_G$  that will mark the transition from a fully turbulent interface to a non-turbulent or intermittent interface can be lower than 0.2 (Fernando, 1991). In consideration of these typical values, it should be reasonable to estimate from Fig. 10 that the interface was fully turbulent for the cases where  $Ri^* = 0.51$ . For the case where  $Ri^* = 1.29$  the interface was probably

characterized partially by Kelvin-Helmholtz waves with some turbulent spots.

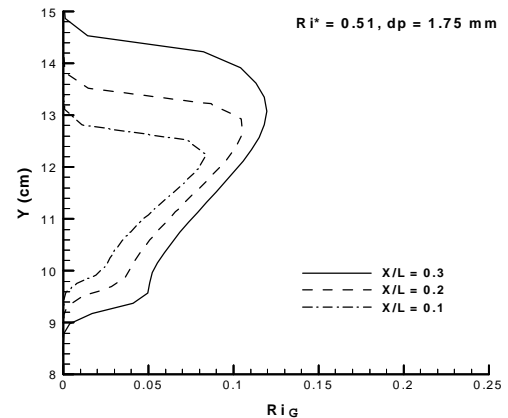


Figure 9 - Gradient Richardson number profiles for case 3.

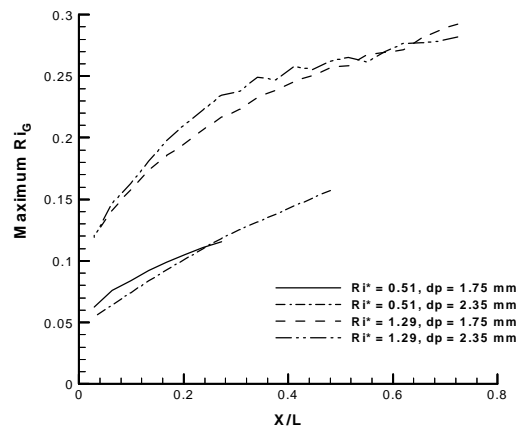


Figure 10 - Maximum gradient Richardson number versus  $x/L$ .

The variation of predicted  $\delta_M$  with  $x/L$  is shown in Fig. 11, along with the variation of the experimentally measured mixed-fluid thickness. It is seen that the SFST model gives reasonable predictions with regard to the trends in the measured  $\delta_M$ . The simulations predict an increasing mixed layer thickness with increasing Richardson number, which is confirmed by the experimental measurements. For the higher Richardson number case, the simulations predict a maximum mixed layer thickness of approximately 2.0 cm, in very good agreement with the experiments. The simulations also show the mixed layer thickness increasing towards 6.0 cm for the lower Richardson number case, which is also in close agreement with the experimental measurements. The sharp change in  $\delta_M$  near the splitter plate is probably due to the inlet conditions, which cause a sharp velocity gradient, which in turn produces a large eddy viscosity at the interface.

How  $\delta_M$  changes with  $x/L$  is interesting because all three flow regimes (see section 1.0) appear to be demonstrated. For the case given by  $Ri^* = 0.51$  and  $d_p = 1.75$  mm, the maximum

gradient Richardson number is approximately 0.1 over the horizontal distance where  $\delta_M$  was calculated for this case. Since this is a low gradient Richardson number, and the effects of the turbulence dominate at the interface,  $\delta_M$  has a slope that is approximately constant. This is characteristic of a mixing layer without density stratification. The effect of the higher slip velocity is to decrease  $\delta_M$ . For  $Ri^* = 0.51$  and  $d_p = 2.35$  mm, the effect of the average droplet size (or the slip velocity) is to bend the curve towards the end as  $x/L$  increases, indicating an inversion of the shear layer.

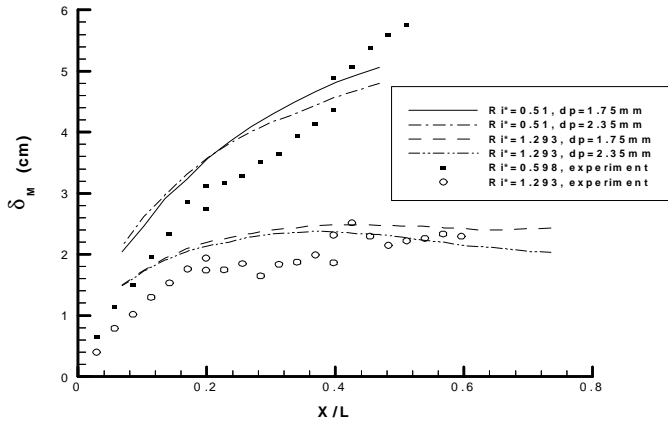


Figure 11 - Mixed fluid thickness versus  $x/L$ .

The influence of the slip velocity is to separate the mixed fluid layers, representing the effect of rising fuel droplets under the action of buoyancy. Initially,  $Ri_G$  is relatively small and the turbulence begins mixing the layers. As  $Ri_G$  increases, the turbulence is damped and  $\delta_m$  does not increase significantly with  $x/L$ . Finally, as the turbulence decreases still more, the slip velocity begins to separate the layers, causing  $\delta_m$  to decrease. This seems to partially originate from the fact that very near the interface, where  $\delta_m$  is measured, the turbulence is more heavily damped by buoyancy effects.

## CONCLUSIONS

In general, the simulations performed with the SFST model give reasonable predictions for the overall flow field and the parameters related to the mixed layer thickness for both miscible and immiscible stratified shear layers. The predicted flow field was confirmed to qualitatively represent the flow field that was observed at the shear flow facility at Johns Hopkins University. This comparison was done using several instantaneous profiles of the mixed interface at various streamwise locations along the shear layer. Average sizes for the droplets and the influence of the zone of re-circulation near the fuel inlet diffuser were also considered. The manner in which  $\delta$  and  $\delta_M$  first increase and then decrease also agrees with what has been observed in the experiments at Johns Hopkins University (Wu and Katz, 1998) at lower Richardson

numbers. Comparison of the trends and magnitudes of the predicted mixed layer thickness also agrees well with the experimental measurements. The slip velocity term plays an important role in the fully turbulent flow regime.

## ACKNOWLEDGMENTS

This work was sponsored by Geo-Centers, Inc. as a subcontract (No.: GC-3062-98-007) under the Naval Research Lab (NRL) contract No.: N00014-96-C-2097. We thank Dr. J. Katz and his students for their collaboration. The contribution of Dr. P. Chang of NSWC-CD in many ways is also appreciated.

## REFERENCES

- Celik, I., and Umbel, M., 1997, "CFD Simulations of a Scalar at a Sheared Density Interface," Proceedings of AEA Technology, International Users Conference '97, Chicago, Illinois, October 6-10, 1997.
- Celik, I., Umbel, M., Wilson, W., Chang, P., and Hill, B., 1998, "Simulation of Transient Flow Inside a Compensated Fuel/Ballast Tank Using Modified Two-Fluid Model," Proceedings of AEA Technology, Users Conference '98, Claymont, Delaware, September 28 - October 2, 1998.
- Fernando, H., 1991, "Turbulent Mixing in Stratified Fluids," *Ann. Rev. of Fluid Mechanics*, Vol. 23, pp. 455-493.
- Ishii, M., 1975, *Thermo-Fluid Dynamic Theory of Two-Phase Flow*, Paris: Eyrolles.
- Katz, J., 1998, Johns Hopkins University, Baltimore, MD, Personal contact.
- Miles, J., 1984, "Richardson number criterion for the stability of stratified shear flow," *Phys. Fluids*, Vol. 29, pp. 3470-3471.
- Rodi, W., 1980, "Turbulence Models and Their Application in Hydraulics - A State-of-the-Art Review," An IAHR (International Association of Hydraulic Research) Publication, Delft, The Netherlands.
- Sullivan, G., 1992, "On Mixing and Transport at a Sheared Density Interface," Ph.D. Dissertation, California Institute of Technology.
- Sullivan, G., and List, J., 1994, "On mixing and transport at a sheared density interface," *Journal of Fluid Mechanics*, Vol. 273, pp. 213-239.
- Tennekes H., and Lumley, J., 1972, *A First Course in Turbulence*, Cambridge: Mass. Inst. of Tech. Press.
- Umbel, M., 1998, "Prediction of Turbulent Mixing at the Interface of Density Stratified, Shear Flows Using CFD," M.S. Thesis, West Virginia University, December.
- Wu, X., and Katz, J., 1998, "On the Flow Structure and Mixing Phenomena In a Fuel-Water Stratified Shear Layer," Proceedings of the 3rd ASME/JSME Joint Fluids Engineering Conference, July 18-23, 1999, San Francisco, California.